

# Charged current quasi elastic scattering of muon neutrino with nuclei

Kapil Saraswat<sup>1</sup>, Prashant Shukla<sup>2,3,\*</sup>, Vineet Kumar<sup>2</sup>,  
Venktesh Singh<sup>1</sup>

<sup>1</sup> Department of Physics, Institute of Science, Banaras Hindu University, Varanasi 221005, India.

<sup>2</sup> Nuclear Physics Division, Bhabha Atomic Research Center, Mumbai 400085, India

<sup>3</sup> Homi Bhabha National Institute, Anushakti Nagar, Mumbai 400094, India.

E-mail: \* pshuklabarc@gmail.com

**Abstract.** We present a study on the charge current quasi elastic scattering of  $\nu_\mu$  from nucleon and nuclei which gives a charged muon in the final state. To describe nuclei, the Fermi Gas model has been used with proposed Pauli suppression factor. The diffuseness parameter of the Fermi distribution has been obtained using experimental data. We also investigate different parametrizations for electric and magnetic Sach's form factors of nucleons. Calculations have been made for CCQES total and differential cross sections for the cases of  $\nu_\mu - N$ ,  $\nu_\mu - {}^{12}C$  and  $\nu_\mu - {}^{56}Fe$  scatterings and are compared with the data for different values of the axial mass. The present model gives excellent description of measured differential cross section for all the systems.

**Keywords:** Neutrino, QES, Axial mass.

PACS numbers: 13.15.+g, 25.70.Bc, 12.15.-y, 23.40.Bw, 25.60.Dz .

## 1. Introduction

The neutrinos produced in the upper atmosphere due to the bombardment of cosmic rays are one of the best tools for the study of neutrino oscillations. There are many ongoing and proposed experiments worldwide to study the phenomena of neutrino oscillations [1, 2, 3, 4, 5, 6]. The neutrinos with energies between 1 to 3 GeV form bulk of the signal in the detector. The neutrino in this energy range can interact with matter by many processes such as quasi elastic scattering, interaction via resonance pion production, and deep inelastic scattering [7]. There is also coherent pion production process in neutrino nucleus scattering [8]. The charge current interactions of neutrinos inside the matter are important since the experiments measure the recoil muon produced in such interactions. The materials like carbon, iron [6] and argon offer a convenient detector media. We present the studies with carbon and iron.

At the lowest neutrino energies, the interactions with nucleon are either elastic or quasi elastic in which the nucleon recoils intact. In the neutral current (NC) elastic scattering, all neutrinos and all anti-neutrinos can scatter off both neutrons and protons:  $\nu + N \rightarrow \nu + N$ . When neutrinos acquire sufficient energy, they can also undergo the charged current interactions:  $\nu_l + n \rightarrow l^- + p$  and  $\bar{\nu}_l + p \rightarrow l^+ + n$ . This is called charged current quasi-elastic scattering (CCQES) as a charged lepton mass is created. CCQES interactions are important to neutrino physics for two reasons. First, the nucleon recoils intact that enables to measure weak nucleon form factors which are difficult to measure in other scattering probes. Second, the two body interaction enables the kinematics to be completely reconstructed (if one ignores two-nucleon contribution) and hence the initial neutrino energy can be determined which is crucial for measuring the oscillation parameters. Thus, a reliable description of the neutrino quasi elastic scattering (QES) processes (particularly on nuclear targets) is essential for precision studies of neutrino oscillation parameters, such as mass splitting and mixing angles [9, 10, 11, 12, 13, 14, 15].

The most popular model for the CCQES calculations is the Llewellyn Smith (LS) model [16]. The Fermi Gas Model [17] with Pauli suppression condition is used in the case of bound nucleon to include nuclear modifications. These models have advantage that they can be readily incorporated into existing neutrino Monte Carlo generators [18] [19, 20, 21], though there exist more sophisticated calculations of quasi elastic scattering such as relativistic distorted-wave impulse approximation [22]. A global analysis [23] of the QES cross sections measured in high energy  $\nu_\mu$  experiments on nuclear targets finds a value of axial mass  $M_A = 0.977 \pm 0.016$  GeV. There are recent measurements of differential and total cross sections for QES of  $\nu_\mu, \bar{\nu}_\mu$  of energies above 4 GeV on carbon by the NOMAD collaboration [24]. The NOMAD analysis of cross sections assuming free nucleon model yields a value of  $M_A = 1.05 \pm 0.02 \pm 0.06$  GeV. The nuclear effects as will be shown here reduce the cross section by 10 % even at higher neutrino energy above 1 GeV which implies that a larger fit value of  $M_A$  is expected if the nuclear effects are included. The QES cross sections for low energy ( $\approx$ ) 1 GeV neutrino scattering on carbon measured by the MiniBooNE detector [25, 26, 27, 28] is 20% larger than the

model calculations. The model calculations of MiniBooNE analysis use a large value of axial mass (1.35 GeV) which increases the total cross section at all energies along with an empirical parameter in the Pauli Blocking condition which decreases the cross section at lower energies [29]. The data from K2K with oxygen target [30] also require a higher value  $M_A = 1.2 \pm 0.12$  GeV.

To get a better description of the cross-section data at low energy, the work in Ref. [31] parametrizes  $M_A$  as a function of energy which results in a higher value of  $M_A$  at low energy. A recent work uses an axial vector form factor obtained from a generalized axial vector meson dominance model with prior uncertainty band [32]. A relativistic Fermi gas model is then used to describe the MiniBooNE data in neutrino energy range from 0.5 to 1.5 GeV within uncertainties. A superscaling approach (SuSA) based on the analysis of electron nucleon scattering improved with relativistic mean field theory effect is used in Ref. [33]. They also study the contribution of two nucleon knockout reaction in neutrino nucleus interaction. The work in Refs. [34, 35] used the empirical SuSA scaling function to describe the CCQE MinibooNE data including 2p2h (two nucleons producing two holes) contributions. The calculations underestimates the data even after adding the 2p2h contributions. In the present work we do not include the 2p2h contribution.

In this work, we calculate the neutrino-nucleon CCQES cross section using Llewellyn Smith model. We also investigate different parametrizations for electric and magnetic Sach's form factors of nucleons. For the cases of nuclei, the Fermi Gas model has been used with Pauli blocking. Calculations have been made for CCQES total and differential cross sections for the case of  $\nu_\mu - N$ ,  $\nu_\mu - {}^{12}C$  and  $\nu_\mu - {}^{56}Fe$  scattering and are compared with the data with the aim of obtaining appropriate value of the axial mass.

## 2. The Model of Neutrino-Nucleon Quasi Elastic Scattering

The charged current quasi elastic (CCQES) neutrino nucleon differential cross section for a nucleon in the rest is given by [16]

$$\frac{d\sigma^{free}}{dQ^2} = \frac{M_N^2 G_F^2 \cos^2 \theta_c}{8\pi E_\nu^2} \left[ A(Q^2) \pm \frac{B(Q^2)(s-u)}{M_N^2} + \frac{C(Q^2)(s-u)^2}{M_N^4} \right] \quad (1)$$

Here,  $M_N$  is the mass of nucleon,  $G_F$  ( $=1.16 \times 10^{-5}$  GeV<sup>-2</sup>) is the Fermi coupling constant and  $\cos \theta_c$  ( $=0.97425$ ) is the Cabibbo angle. In terms of the mandelstam variables  $s$  and  $u$ , the relation  $s - u = 4M_N E_\nu - Q^2 - m_l^2$ , where  $m_l$  is the mass of muon,  $E_\nu$  is the neutrino energy and  $Q^2$  is the square of the momentum transfer from neutrino to outgoing muon.

The functions  $A$ ,  $B$  and  $C$  can be written in the following form [16]

$$A(Q^2) = \frac{(m_l^2 + Q^2)}{M_N^2} \left\{ \left[ (1 + \tau)F_A^2 - (1 - \tau)(F_1^V)^2 \right. \right. \\ \left. \left. + \tau(1 - \tau)(F_2^V)^2 + 4\tau F_1^V F_2^V \right] \right\}$$

$$- \frac{m_l^2}{4M_N^2} \left[ (F_1^V + F_2^V)^2 + (F_A + 2F_P)^2 - 4(1 + \tau)F_P^2 \right] \}, \quad (2)$$

$$B(Q^2) = \frac{Q^2}{M_N^2} F_A (F_1^V + F_2^V), \quad (3)$$

$$C(Q^2) = \frac{1}{4} \left[ F_A^2 + (F_1^V)^2 + \tau(F_2^V)^2 \right]. \quad (4)$$

Here,  $\tau = Q^2/(4M^2)$ . The form factors used for neutrino and antineutrino scatterings are the same because of the charge symmetry of the matrix element. The function  $F_A$  is the axial form factor,  $F_P$  is the pseudoscalar form factor and  $F_1^V, F_2^V$  are the vector form factors.

The axial form factor  $F_A$  can be written in the dipole form [36] as

$$F_A(Q^2) = \frac{g_A}{\left(1 + \frac{Q^2}{M_A^2}\right)^2}, \quad (5)$$

where  $g_A (= -1.267)$  is the axial vector constant and  $M_A$  is the axial mass. The pseudoscalar form factor  $F_P$  can be calculated from the axial form factor  $F_A$  [37] as

$$F_P(Q^2) = \frac{2 M_N^2}{Q^2 + m_\pi^2} F_A(Q^2), \quad (6)$$

where  $m_\pi$  is the mass of pion. The vector form factors  $F_1^V$  and  $F_2^V$  can be written as [36] [38]

$$F_1^V = \frac{\left[ G_E^p(Q^2) - G_E^n(Q^2) \right] + \tau \left[ G_M^p(Q^2) - G_M^n(Q^2) \right]}{1 + \tau}, \quad (7)$$

$$F_2^V = \frac{\left[ G_M^p(Q^2) - G_M^n(Q^2) \right] - \left[ G_E^p(Q^2) - G_E^n(Q^2) \right]}{1 + \tau}. \quad (8)$$

Here,  $G_E^{p,n}$  and  $G_M^{p,n}$  are respectively the electric and magnetic Sach's form factors of nucleons (proton and neutron). There are many parametrizations of these form factors which are obtained by fitting the electron scattering data and are given by Galster [39], Budd et al. [40], Bradford et al. [41], Bosted [42] and Alberico et al. [43]. We use Galster parametrizations in our calculation. We find that all the parametrizations produce almost same results. Such a comparison with Galster and the latest Alberico's parametrizations is presented in the results section.

The electric and magnetic Sach's form factors given by Galster [39] are as follows

$$\begin{aligned} G_E^p &= G_D(Q^2), \\ G_M^p(Q^2) &= \mu_p G_D(Q^2), \\ G_M^n(Q^2) &= \mu_n G_D(Q^2). \end{aligned} \quad (9)$$

For the electric form factor of neutron, we use the parametrization given by Krutov et. al. [44] as

$$G_E^n(Q^2) = -\mu_n \frac{0.942 \tau}{(1 + 4.61 \tau)} G_D(Q^2). \quad (10)$$

The magnetic moment of proton  $\mu_p = 2.793$  and that of neutron  $\mu_n = -1.913$ . The dipole form factor  $G_D(Q^2)$  is given by [36]

$$G_D(Q^2) = \frac{1}{\left(1 + \frac{Q^2}{M_\pi^2}\right)^2}, \quad (11)$$

with  $M_\pi^2 = 0.71 \text{ GeV}^2$ .

The Sach's form factor given by Alberico et al. [43] are

$$\begin{aligned} G_E^p(Q^2) &= \frac{1 - 0.14\tau}{1 + 11.18\tau + 15.18\tau^2 + 23.57\tau^3}, \\ \frac{G_M^p(Q^2)}{\mu_p} &= \frac{1 + 1.07\tau}{1 + 12.30\tau + 25.43\tau^2 + 30.39\tau^3}, \\ G_E^n(Q^2) &= -\frac{0.10}{(1 + 2.83Q^2)^2} + \frac{0.10}{(1 + 0.43Q^2)^2}, \\ \frac{G_M^n(Q^2)}{\mu_n} &= \frac{1 + 2.13\tau}{1 + 14.53\tau + 22.76\tau^2 + 78.29\tau^3}. \end{aligned} \quad (12)$$

We study the effect of Galster and Alberico parametrizations of electromagnetic form factors on CCQES cross section of neutrino nucleon scattering.

The neutrino QES total cross section for a free nucleon is calculated as [45]

$$\sigma^{free}(E_\nu) = \int_{Q_{min}^2}^{Q_{max}^2} dQ^2 \frac{d\sigma^{free}(E_\nu, Q^2)}{dQ^2}, \quad (13)$$

where

$$\begin{aligned} Q_{min}^2 &= -m_l^2 + 2 E_\nu (E_l - |\vec{k}'|) \\ &= \frac{2E_\nu^2 M_N - M_N m_l^2 - E_\nu m_l^2 - E_Q}{2E_\nu + M_N}, \end{aligned} \quad (14)$$

$$\begin{aligned} Q_{max}^2 &= -m_l^2 + 2 E_\nu (E_l + |\vec{k}'|) \\ &= \frac{2E_\nu^2 M_N - M_N m_l^2 + E_\nu m_l^2 + E_Q}{2E_\nu + M_N}, \end{aligned} \quad (15)$$

where  $E_Q = E_\nu \sqrt{(s - m_l^2)^2 - 2(s + m_l^2)M_N^2 + M_N^4}$ ,  $s = M_N^2 + 2M_N E_\nu$  and  $E_l$  and  $\vec{k}'$  are the energy and momentum of the charged lepton.

### The Fermi Gas Model

The cross section for the neutrino scattering with a nucleon in a nucleus is smaller than that in the case of free nucleon scattering. The nucleus can be treated in terms of the Fermi gas model where the nucleons move independently (Fermi motion) within the nuclear volume in a constant binding potential generated by all nucleons. In the Fermi gas model, all the states up to the Fermi momentum  $k_F$  are occupied. The Pauli blocking implies that the cross section for all the interactions leading to a final state nucleon with a momentum smaller than  $k_F$  is equal to zero. There are many prescriptions for the Fermi model [16, 17, 23] and Pauli blocking.

The differential cross section per neutron for the charged current neutrino-nucleus quasi elastic scattering is given by

$$\frac{d\sigma^{nucleus}(E_\nu)}{dQ^2} = \frac{2V}{(A-Z)(2\pi)^3} \int_0^\infty 2\pi k_n^2 dk_n d(\cos\theta) f(\vec{k}_n) S(\nu - \nu_{min}) \frac{d\sigma^{free}(E_\nu^{eff}(E_\nu, \vec{k}_n))}{dQ^2}. \quad (16)$$

Here, the factor 2 accounts for the spin of the neutron,  $2V/((A-Z)(2\pi)^3) = \rho_0$  and  $V$  is the volume of the the nucleus.  $d\sigma^{free}/dQ^2$  is the neutrino QES differential cross section for free neutron at rest given by Eq. 1. The effective neutrino energy  $E_\nu^{eff}$  in the presence of the Fermi motion of the nucleon is given by

$$E_\nu^{eff} = \frac{(s^{eff} - M_n^2)}{2M_n}. \quad (17)$$

Here,  $s^{eff} = M_n^2 + 2E_\nu(E_n - k_n \cos(\theta))$  and the neutron energy is  $E_n = \sqrt{k_n^2 + M_n^2}$  in terms of neutron momentum  $k_n$  and mass  $M_n$ . The fermi distribution for non-interacting particles at zero temperature sharply drops at fermi momentum. In reality, the fermi distribution would drop smoothly with a diffuseness  $a = kT$ . The Fermi distribution function  $f(\vec{k}_n)$  is defined as

$$f(k_n) = \frac{1}{1 + \exp(\frac{k_n - k_F}{a})}. \quad (18)$$

Here,  $k_F$  is the mean Fermi momentum. The normalization  $\rho_0$  is given as

$$\rho_0 = \frac{1}{\frac{4\pi}{3} k_F^3 \left(1 + \frac{\pi^2 a^2}{k_F^2}\right)}. \quad (19)$$

The Pauli suppression factor is given by

$$S(\nu - \nu_{min}) = \frac{1}{1 + \exp(-\frac{(\nu - \nu_{min})}{a})}. \quad (20)$$

Here, the variable  $\nu = (Q^2 + M_p^2 - M_n^2)/(2M_n)$  is the energy transfer in the collisions and  $\nu_{min}$  is obtained by Pauli Blocking and binding energy ( $E_B$ ) considerations:  $\nu_{min} = \sqrt{k_F^2 + M_p^2} - \sqrt{k_n^2 + M_n^2} + E_B$ . The value of binding energy is 10 MeV for both carbon and iron nuclei. The  $Q^2$  is restricted in  $Q_{min}^2 < Q^2 < Q_{max}^2$  where  $Q_{min}^2$  and  $Q_{max}^2$  are calculated by Eq. 14 and 15 but with  $E_\nu^{eff}$ .

The value of the Fermi momentum ( $k_F$ ) for the carbon nucleus is taken as 0.221 GeV from Ref. [46]. For the iron nucleus,  $k_F$  for both the neutron and proton is taken as 0.260 GeV from Ref. [46].

### 3. Results and Discussions

Figure 1 shows the electric Sach's form factor  $G_E^p$  for proton as a function of square of momentum transfer  $Q^2$  obtained using Galster and Alberico parametrizations. Both the parametrizations give very similar values of  $G_E^p$  but at  $Q^2 \gtrsim 1 \text{ GeV}^2$  Galster's

values are slightly above the Alberico's values. Figure 2 shows the magnetic Sach's form factor  $G_M^p$  for proton as a function of  $Q^2$  obtained using Galster and Alberico parametrization. Both the parametrizations give very similar values of  $G_M^p$  and for  $Q^2 \gtrsim 1 \text{ GeV}^2$  Galster's values are slightly below Alberico values. Figure 3 shows the electric Sach's form factor  $G_E^n$  for neutron as a function of  $Q^2$  obtained using Galster and Alberico parametrization. Below  $Q^2 \approx 1 \text{ GeV}^2$ , the values of the Galster parametrization is more than that from Alberico parametrization but above  $Q^2 \approx 1 \text{ GeV}^2$ , the Alberico parametrization gives higher values. Figure 4 shows the magnetic Sach's form factor  $G_M^n$  for neutron as a function  $Q^2$  obtained using the Galster and Alberico parametrization. Both the parametrizations give almost same values of  $G_M^n$ . In the Ref. [47], the authors study various parameterizations of Galster et al. [39], Budd et al. [40], Bradford et al. [41], Bosted et al. [42] and Alberico et al. [43] to observe their effect on scattering cross sections for neutrino induced CCQES processes on nuclear target like Ar. They found that the cross section has no dependence on the choice of parameterizations at  $E_\nu < 1 \text{ GeV}$ .

Figure 5 shows the differential cross section  $d\sigma/dQ^2$  for the neutrino-neutron CCQES as a function of  $Q^2$  obtained using Galster (at  $M_A = 0.979, 1.05, 1.12$  and  $1.23 \text{ GeV}$ ) and Alberico (at  $M_A = 1.12 \text{ GeV}$ ) parametrization at  $2 \text{ GeV}$  neutrino energy. The value of  $d\sigma/dQ^2$  increases with the increase in the value of axial mass  $M_A$ . A comparison of the cross sections using the Alberico and the Galster parametrizations made at axial mass  $M_A = 1.12 \text{ GeV}$  shows that there is no noticeable difference due to different parametrizations of Sach's form factors and for all further calculations we use the Galster parametrization. Such a study has been made with all the parameterizations as mentioned in the last section and these do not make any difference to the cross section.

Figure 6 shows the differential cross section  $d\sigma/dQ^2$  for the neutrino-neutron, neutrino-carbon and neutrino-iron CCQES as a function of  $Q^2$  at  $2 \text{ GeV}$  neutrino energy obtained using axial mass  $M_A = 1.05 \text{ GeV}$ . For the neutrino-carbon and neutrino-iron calculations we use the Fermi Gas model with Pauli blocking. The Fermi momentum ( $k_F$ ) for the carbon nucleus is taken as  $0.221 \text{ GeV}$  and for the iron nucleus it is taken as  $0.260 \text{ GeV}$ . The effective binding energy  $E_B$  of nucleon in the nucleus is taken as  $10 \text{ MeV}$ . The value of  $a$  is  $0.020 \text{ GeV}$ . The cross sections at low  $Q^2$  drop due to the nuclear effects. Due to diffuseness parameter, the differential cross-section for neutrino nucleus interaction drops smoothly as  $Q^2$  goes to zero as shown in Fig. 6.

Figure 7 shows the differential cross section  $d\sigma/dQ^2$  per neutron for the neutrino-carbon CCQES as a function of  $Q^2$  at different values of axial mass  $M_A = 0.979, 1.05, 1.12$  and  $1.23 \text{ GeV}$  using Galster parametrizations for Sach's form factors. The calculations correspond to an average neutrino energy  $\langle E_\nu \rangle = 0.788 \text{ GeV}$  are compared with the data recorded by the MiniBooNE (MiniBooNE10) experiment [29]. The cross section is obtained by averaging over calculations in a range of energies weighted by the neutrino energy spectrum given by the MiniBooNE data. The calculations with  $M_A = 1.05, 1.12$  and  $1.23 \text{ GeV}$  are compatible with the data.

Figure 8 shows the differential cross section  $d\sigma/dQ^2$  per neutron for the neutrino-

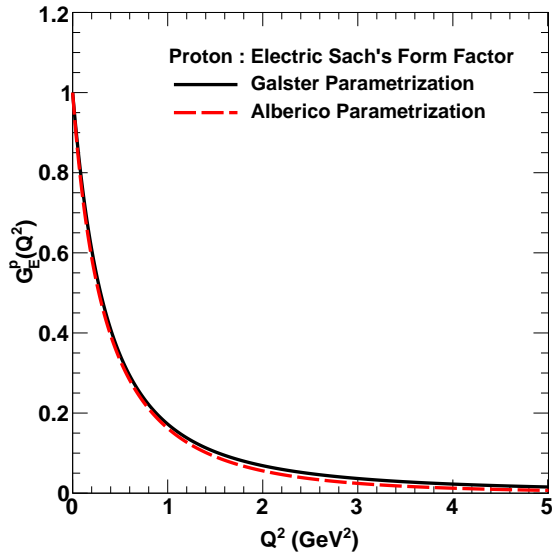


Figure 1. Electric Sach's form factor  $G_E^p$  for proton as a function of  $Q^2$ .

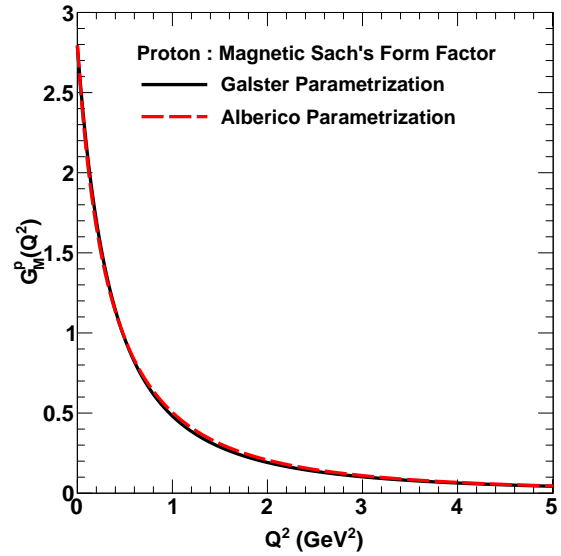


Figure 2. Magnetic Sach's form factor  $G_M^p$  for proton as a function of  $Q^2$ .

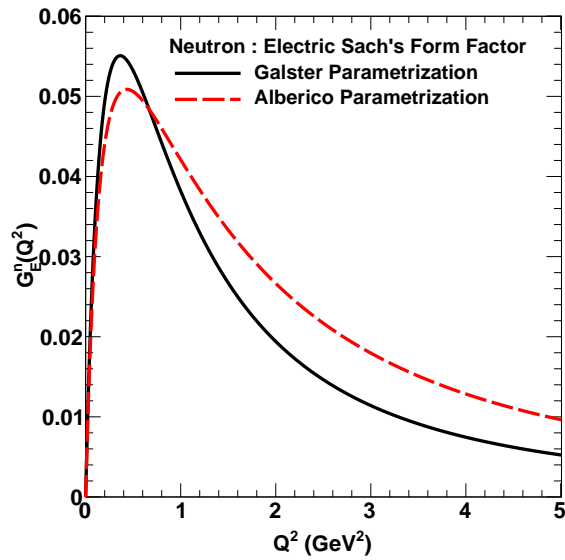


Figure 3. Electric Sach's form factor for  $G_E^n$  neutron as a function of  $Q^2$ .

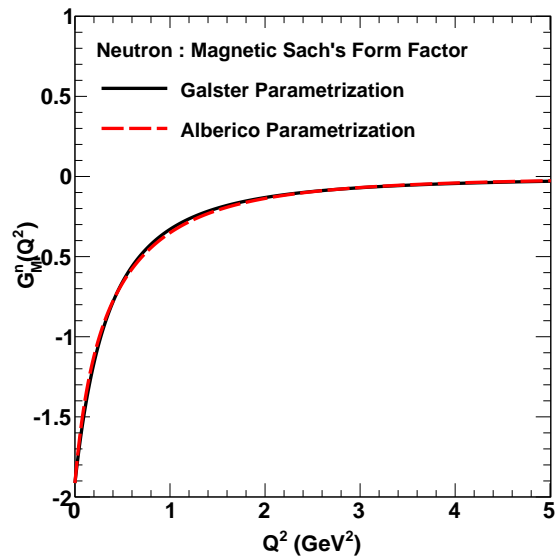
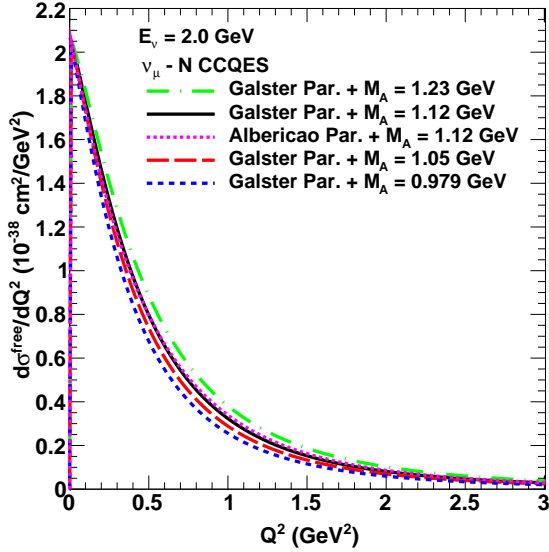
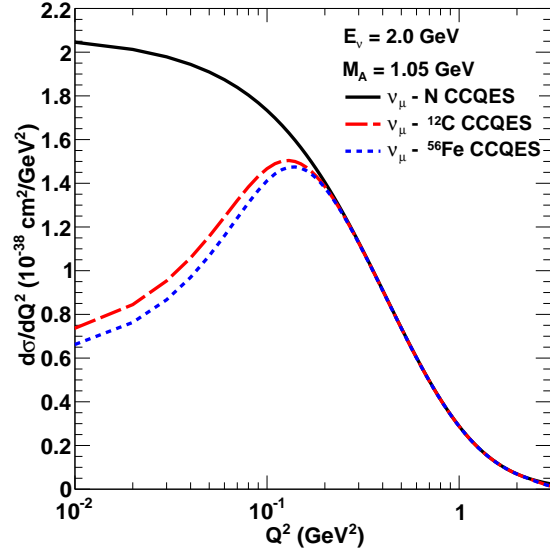


Figure 4. Magnetic Sach's form factor for  $G_M^n$  neutron as a function of  $Q^2$ .





**Figure 5.** Differential cross section  $d\sigma/dQ^2$  for the neutrino-neutron CCQES as a function of  $Q^2$  at neutrino energy  $E_\nu = 2$  GeV for different values of the axial mass  $M_A$ .



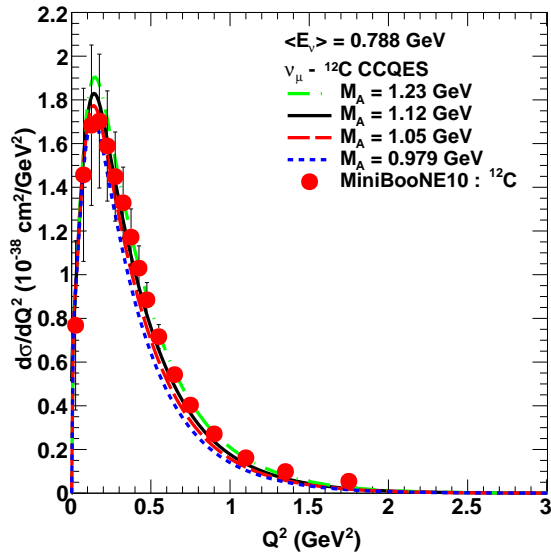
**Figure 6.** Differential cross section  $d\sigma/dQ^2$  for  $\nu_\mu - N$ ,  $\nu_\mu - {}^{12}\text{C}$  and  $\nu_\mu - {}^{56}\text{Fe}$  CCQES as a function of  $Q^2$  at neutrino energy  $E_\nu = 2$  GeV for axial mass  $M_A = 1.05$  GeV.

carbon CCQES as a function of  $Q^2$  with different values of  $M_A = 0.979, 1.05, 1.12$  and  $1.23$  GeV. The calculations are at an average neutrino energy  $\langle E_\nu \rangle = 2$  GeV corresponding to the data recorded by the GGM77 (Gargamelle) [48]. The cross section from GGM79 experiment [49] measured in the neutrino energy range  $1.5$  to  $5.5$  GeV are also plotted. The calculations with  $M_A = 0.979$  and  $1.05$  GeV are compatible with the data.

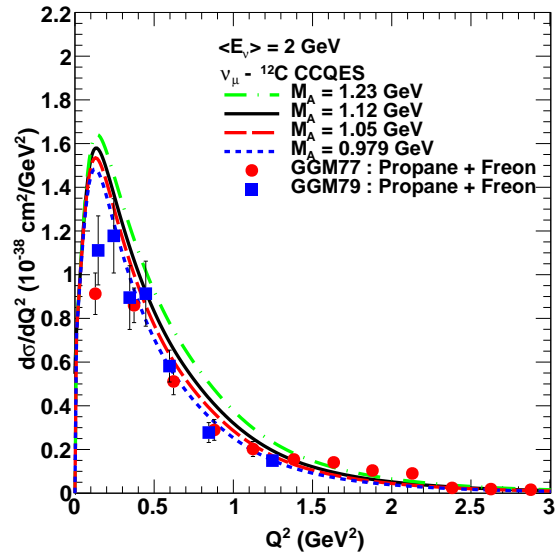
Figure 9 shows the differential cross section  $d\sigma/dQ^2$  per neutron for the neutrino-carbon CCQES as a function of  $Q^2$  with values of  $M_A = 0.979, 1.05, 1.12$  and  $1.23$  GeV. The calculations are at average neutrino energy  $\langle E_\nu \rangle = 3.5$  GeV corresponding to the MINER $\nu$ A data [50]. The calculations with  $M_A = 1.05$  and  $1.12$  GeV are compatible with the data.

Figure 10 predicts the differential cross section  $d\sigma/dQ^2$  per neutron for the neutrino-iron CCQES as a function of the square of momentum transfer  $Q^2$  at neutrino energy  $2$  GeV for values of  $M_A = 0.979, 1.05, 1.12$  and  $1.23$  GeV.

Figure 11 shows the total cross section  $\sigma$  for the neutrino - neutron CCQES as a function of  $E_\nu$  obtained using Galster (at  $M_A = 0.979, 1.05, 1.12$  and  $1.23$  GeV) and Alberico (at  $M_A = 1.12$  GeV) parametrization. The value of  $\sigma$  increases with the increase in the value of axial mass  $M_A$ . A comparison of the total cross sections using the Alberico parametrizations and the Galster parametrization made at axial mass  $M_A = 1.12$  GeV shows that there is no noticeable difference due to different parametrizations of Sach's form factors. The calculations are compared with the



**Figure 7.** Differential cross section  $d\sigma/dQ^2$  per neutron for the neutrino-carbon CCQES as a function of  $Q^2$  for different values of the axial mass  $M_A$  at an average neutrino energy  $\langle E_\nu \rangle = 0.788$  GeV corresponding to MiniBooNE data [29].

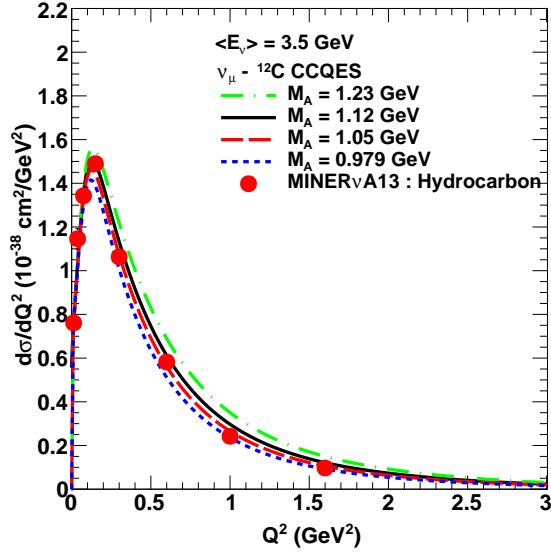


**Figure 8.** Differential cross section  $d\sigma/dQ^2$  per neutron for the neutrino-carbon CCQES as a function of  $Q^2$  for different values of the axial mass  $M_A$  at average neutrino energy  $\langle E_\nu \rangle = 2$  GeV corresponding to GGM data [48, 49].

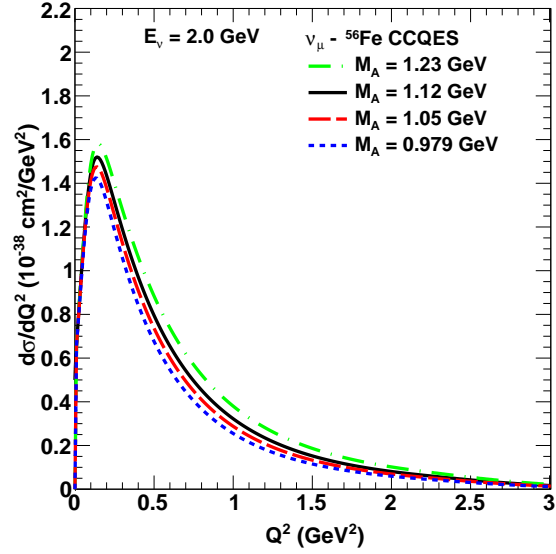
data recorded by Neutrino Oscillation Magnetic Detector (NOMAD09) [24], Argonne National Laboratory (ANL73) [51], Argonne National Laboratory (ANL77) [52], Brookhaven National Laboratory (BNL81) [53], Fermi National Laboratory (FNAL83) [54] and Big European Bubble Chamber (BEBC90) [55] collaboration. The calculations with  $M_A = 0.979, 1.05$  and  $1.12$  GeV are compatible with the data. The calculations of  $\sigma$  with  $M_A = 1.23$  GeV overestimate all the experimental data. The diffuseness parameter does not affect the total cross section.

Figure 12 shows the total cross section  $\sigma$  for the neutrino-neutron, neutrino-carbon and neutrino-iron CCQES as a function of  $E_\nu$  obtained using axial mass  $M_A = 1.05$  GeV. For the neutrino-carbon and neutrino-iron calculations we use the Fermi Gas model with Pauli blocking. The nuclear effects reduce the cross section by 10 % even at higher neutrino energy above 1 GeV.

Figure 13 shows the total cross section  $\sigma$  per neutron for the neutrino-carbon CCQES scattering as a function of  $E_\nu$  obtained using Galster parametrization with axial mass  $M_A = 0.979, 1.05, 1.12$  and  $1.23$  GeV. The calculations are compared with the data recorded by NOMAD09 [24], MiniBooNE10 [29], GGM77 [48], GGM79 [49] and SKAT90 [56] experiments. The calculations with the value of  $M_A = 1.23$  GeV describes the MiniBooNE data but overestimate the other experimental data. The calculations with  $M_A = 1.05$  and  $1.12$  GeV are compatible with NOMAD09, GGM77, GGM79 and



**Figure 9.** Differential cross section  $d\sigma/dQ^2$  per neutron for the neutrino-carbon CCQES as a function of  $Q^2$  for different values of the axial mass  $M_A$  at average neutrino energy  $\langle E_\nu \rangle = 3.5$  GeV corresponding to MINER $\nu$ A data [50].



**Figure 10.** Differential cross section  $d\sigma/dQ^2$  per neutron for the neutrino-iron CCQES as a function of  $Q^2$  at neutrino energy  $E_\nu = 2$  GeV for different values of the axial mass  $M_A$ .

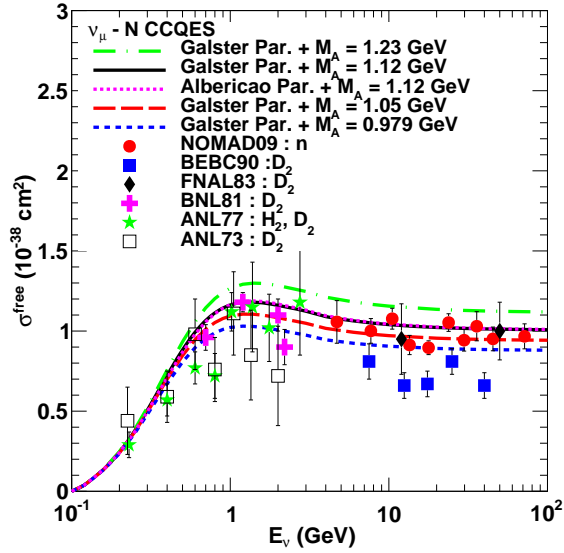


**Figure 11.** Total cross section  $\sigma$  for the neutrino-neutron CCQES as a function of neutrino energy  $E_\nu$  for different values of the axial mass  $M_A$  compared with the data [24, 51, 52, 53, 54, 55]

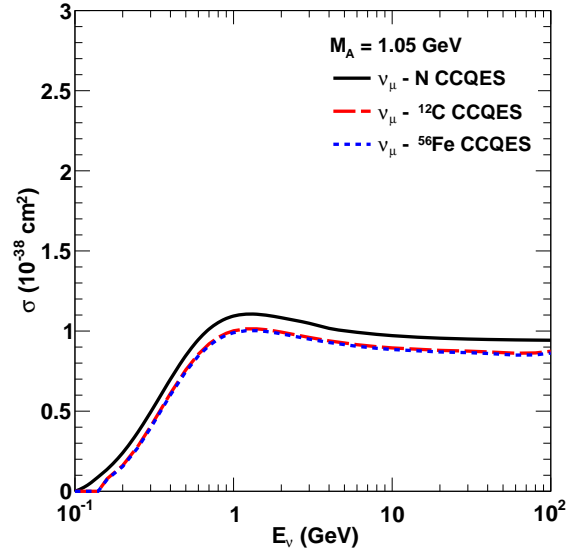


**Figure 12.** Total cross section  $\sigma$  for  $\nu_\mu-N$ ,  $\nu_\mu-^{12}C$  and  $\nu_\mu-^{56}Fe$  CCQES as a function of neutrino energy  $E_\nu$  for axial mass  $M_A = 1.05$  GeV.

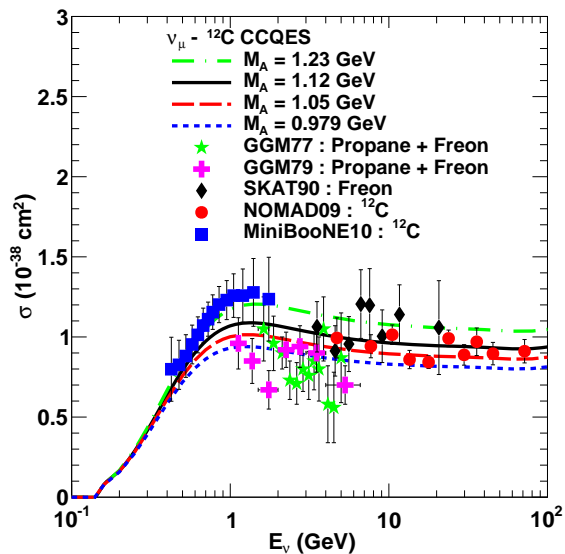


**Figure 13.** Total cross section  $\sigma$  per neutron for the neutrino-carbon charged current quasi elastic scattering as a function of neutrino energy  $E_\nu$  for different values of the axial mass  $M_A$  compared with the data [24, 29, 48, 49, 56].

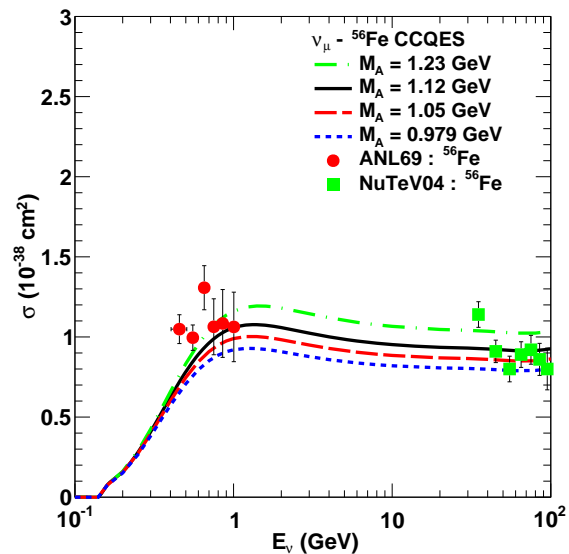


**Figure 14.** Total cross section  $\sigma$  per neutron for the neutrino-iron charged current quasi elastic scattering as a function of neutrino energy  $E_\nu$  for different values of the axial mass  $M_A$  compared with the data [57, 58].

SKAT90 data. There are alternative ways to get a better description of the cross-section data at low energy e.g. the work in Ref. [31] parametrizes  $M_A$  as a function of energy which results in higher value of  $M_A$  at low energy.

Figure 14 shows the total cross section  $\sigma$  per neutron for the neutrino-iron CCQES as a function of the  $E_\nu$  obtained using Galster parametrization with axial mass  $M_A = 0.979, 1.05, 1.12$  and  $1.23$  GeV. The calculations are compared with the data recorded by ANL69 [57] and Neutrino at the Tevatron (NuTeV04) [58] experiments. The calculations with  $M_A = 1.05$  and  $1.12$  GeV are compatible with the data.

#### 4. Conclusion

We presented a study on the charge current quasi elastic scattering of  $\nu_\mu$  from nucleon and nuclei. We use a Fermi model with Pauli suppression factor which is simple to incorporate yet includes all the essential features. The investigation of parametrizations for electric and magnetic Sach's form factors of nucleons shows that there is no noticeable difference in cross section due to different parametrizations. Calculations have been made for CCQES total and differential cross sections for the cases of  $\nu_\mu - N$ ,  $\nu_\mu - {}^{12}\text{C}$  and  $\nu_\mu - {}^{56}\text{Fe}$  scatterings and are compared with the data for different values of the axial mass. The calculations give excellent description of the differential cross section

data. The diffuseness parameter does not affect the total cross section. The calculations with axial mass 1.05 and 1.12 GeV give good description of most of the experimental data and thus a value between these two can be taken as the most acceptable value of  $M_A$ . The data from MiniBooNE demands a larger value of  $M_A = 1.23$  GeV to get an excellent fit.

## References

- [1] Y Ashie *et al* [Super-Kamiokande Collaboration] *Phys. Rev. D* **71** 112005 (2005).
- [2] Y Takeuchi [Super-Kamiokande Collaboration] *Nucl. Phys. Proc. Suppl.* **229-232** 79 (2012).
- [3] E Aliu *et al* [K2K Collaboration] *Phys. Rev. Lett.* **94** 081802 (2005).
- [4] M H Ahn *et al* [K2K Collaboration] *Phys. Rev. Lett.* **90** 041801 (2003).
- [5] M H Ahn *et al* [K2K Collaboration] *Phys. Rev. D* **74** 072003 (2006).
- [6] S Ahmed *et al.* [ICAL Collaboration] *Pramana* **88** 79 (2017).
- [7] J A Formaggio and G P Zeller *Rev. Mod. Phys.* **84** 1307 (2012).
- [8] K Saraswat, P Shukla, V Kumar and V Singh *Phys. Rev. C* **93** 035504 (2016).
- [9] S Fukuda *et al* [Super-Kamiokande Collaboration] *Phys. Rev. Lett.* **85** 3999 (2000).
- [10] D G Michael *et al* [MINOS Collaboration] *Phys. Rev. Lett.* **97** 191801 (2006).
- [11] P Adamson *et al* [MINOS Collaboration] *Phys. Rev. D* **81** 072002 (2010).
- [12] P Adamson *et al* [MINOS Collaboration] *Phys. Rev. Lett.* **107** 021801 (2011).
- [13] P Adamson *et al* [NOvA Collaboration] *Phys. Rev. Lett.* **116** 151806 (2016),
- [14] P Adamson *et al* [NOvA Collaboration] *Phys. Rev. D* **93** 051104 (2016).
- [15] P Adamson *et al* [NOvA Collaboration] *Phys. Rev. Lett.* **118** 151802 (2017).
- [16] C H Llewellyn Smith *Phys. Rept.* **3** 261 (1972).
- [17] R A Smith and E J Moniz *Nucl. Phys. B* **43** 605 (1972) Erratum: *Nucl. Phys. B* **101** 547 (1975).
- [18] C Andreopoulos *et al* *Nucl. Instrum. Meth. A* **614** 87 (2010).
- [19] H Gallagher *Nucl. Phys. Proc. Suppl.* **112** 188 (2002).
- [20] Y Hayato *Nucl. Phys. Proc. Suppl.* **112** 171 (2002).
- [21] D Casper *Nucl. Phys. Proc. Suppl.* **112** 161 (2002).
- [22] A V Butkevich *Phys. Rev. C* **82** 055501 (2010).
- [23] K S Kuzmin, V V Lyubushkin and V A Naumov *Eur. Phys. J. C* **54** 517 (2008).
- [24] V Lyubushkin *et al* [NOMAD Collaboration] *Eur. Phys. J. C* **63** 355 (2009).
- [25] A A Aguilar-Arevalo *et al* [MiniBooNE Collaboration] *Phys. Rev. Lett.* **98** 231801 (2007).
- [26] A A Aguilar-Arevalo *et al* [MiniBooNE Collaboration] *Phys. Rev. D* **84** 072005 (2011).
- [27] C Juszczak, J T Sobczyk and J Zmuda *Phys. Rev. C* **82** 045502 (2010).
- [28] A A Aguilar-Arevalo *et al* [MiniBooNE Collaboration] *Phys. Rev. D* **82** 092005 (2010).
- [29] A A Aguilar-Arevalo *et al* [MiniBooNE Collaboration] *Phys. Rev. D* **81** 092005 (2010).
- [30] R Gran *et al* [K2K Collaboration] *Phys. Rev. D* **74** 052002 (2006).
- [31] L D Kolupaeva, K S Kuzmin, O N Petrova and I M Shandrov *Mod. Phys. Lett. A* **31** 1650077 (2016).
- [32] J E Amaro and E Ruiz Arriola *Phys. Rev. D* **93** 053002 (2016).
- [33] G D Megias, J E Amaro, M B Barbaro, J A Caballero, T W Donnelly and I Ruiz Simo *Phys. Rev. D* **94** 093004 (2016) .
- [34] J E Amaro, M B Barbaro, J A Caballero, T W Donnelly and C F Williamson *Phys. Lett. B* **696** 151 (2011).
- [35] J E Amaro, M B Barbaro, J A Caballero and T W Donnelly *Phys. Rev. Lett.* **108** 152501 (2012).
- [36] P Stoler *Phys. Rept.* **226** 103 (1993).
- [37] V Bernard, L Elouadrhiri and U G Meissner *J. Phys. G* **28** R1 (2002).
- [38] H S Budd, A Bodek and J Arrington *hep-ex/0308005*.

- [39] S Galster, H Klein, J Moritz, K H Schmidt, D Wegener and J Bleckwenn *Nucl. Phys. B* **32** 221 (1971).
- [40] H S Budd, A Bodek and J Arrington *Nucl. Phys. Proc. Suppl.* **139** 90 (2005).
- [41] R Bradford, A Bodek, H S Budd and J Arrington, *Nucl. Phys. Proc. Suppl.* **159** 127 (2006).
- [42] P E Bosted *Phys. Rev. C* **51** 409 (1995).
- [43] W M Alberico, S M Bilenky, C Giunti and K M Graczyk *Phys. Rev. C* **79** 065204 (2009).
- [44] A F Krutov and V E Troitsky, *Eur. Phys. J. A* **16** 285 (2003).
- [45] Amin A Leghrouz, M A Abu-Samreh and A M Saleh *J Al-Aqsa Univ.* **10(S.E.)** (2006).
- [46] E J Moniz, I Sick, R R Whitney, J R Ficenec, R D Kephart and W P Trower *Phys. Rev. Lett.* **26** 445 (1971).
- [47] F. Akbar, M. Rafi Alam, M. Sajjad Athar, S. Chauhan, S. K. Singh and F. Zaidi, *Int. J. Mod. Phys. E* **24** 1550079 (2015).
- [48] S Bonetti *et al* *Nuovo Cim. A* **38** 260 (1977).
- [49] M Pohl *et al* [GARGAMELLE NEUTRINO PROPANE Collaboration] *Lett. Nuovo Cim.* **26** 332 (1979).
- [50] G A Fiorentini *et al* [MINERvA Collaboration] *Phys. Rev. Lett.* **111** 022502 (2013).
- [51] W A Mann *et al* *Phys. Rev. Lett.* **31** 844 (1973).
- [52] S J Barish *et al* *Phys. Rev. D* **16** 3103 (1977).
- [53] N J Baker *et al* *Phys. Rev. D* **23** 2499 (1981).
- [54] T Kitagaki *et al* *Phys. Rev. D* **28** 436 (1983).
- [55] D Allasia *et al* *Nucl. Phys. B* **343** 285 (1990).
- [56] J Brunner *et al* [SKAT Collaboration] *Z. Phys. C* **45** 551 (1990).
- [57] R L Kustom, D E Lundquist, T B Novey, A Yokosawa and F Chilton *Phys. Rev. Lett.* **22** 1014 (1969).
- [58] N Suwonjandee *FERMILAB-THESIS-2004-67 UMI-31-20857* University of Cincinnati.